Oblique shock waves in non-ideal compressible flows

Davide Vimercati[1], Giulio Gori[2], Alfred Kluwick[3], Alberto Guardone[4],

[1] *Universität der Bundeswehr München, 85577 Neubiberg, Germany*
[2] *Centre Inria Saclay – Île-de-France, 91120 Palaiseau, France*
[3] *Technische Universität Wien, 1060 Vienna, Austria*
[4] *Politecnico di Milano, 20156 Milan, Italy*

Abstract

The nature of shock waves is dictated by the values of the thermodynamic parameter Γ, known as the fundamental derivative of gasdynamics, which expresses the variation of the speed of sound with the density at constant entropy. Flows evolving in a region where $\Gamma < 0$ allow for expansion shock waves only (i.e. the fluid particles experience a decrease in pressure as the shock front is crossed) to be formed, in contrast to the conventional, compressive shocks if $\Gamma > 0$. In the mixed regime where Γ can change its sign, so-called sonic shocks, having unitary normal Mach number relative to the front, can also be formed. Within the context of single-phase steady flows, the present work provides an overview of the non-ideal effects that characterise shock waves occurring in fluids having $\Gamma < 1$. Three main topics are covered: the increase of the Mach number across the shock, the formation of expansion and sonic shocks and finally anomalies in the interaction of shock waves.

1 Introduction

The states far upstream and downstream of an isolated shock wave, i.e. the states immediately upstream and downstream of the shock front in the inviscid limit of the equation of fluid dynamics, are related via the well-known Rankine-Hugoniot relations (see, e.g, [1]). In the case of ideal gases with constant specific heats (i.e. for gases at sufficiently high temperatures and low pressures) closed-form expressions for the fluid states on each side of the shock can be obtained. From the qualitative point of view, from these formula it follows that the pressure, density, temperature and entropy increase, while the Mach number decreases, in passing through the shock. A number of discrepancies from this ideal picture of shock waves can be traced back to anomalies, i.e. a *non-ideal* behaviour, in the speed of sound.

To fix ideas, let us focus our attention on a steady supersonic stream having given values of pressure P_A, specific volume v_A and Mach number $M_A \geq 1$, together with the flow direction. An oblique shock brings the flow from the given (pre-shock) state to another state characterised by P_B, v_B, M_B (post-shock state). Assuming that the pressure jump $[P] = P_B - P_A$ is small and $\Gamma = \mathcal{O}(1)$, the Taylor series expansion for the post-shock entropy and Mach number can be written as [2, 3]

$$s_B = s_A + \frac{\Gamma_A}{6T_A}\frac{[P]^3}{\rho_A^3 c_A^4} + \mathcal{O}\left([P]^4\right) \tag{1}$$

and

$$\frac{M_B}{M_A} = 1 + \left(1 - \Gamma_A - \frac{1}{M_A^2}\right)\frac{[P]}{\rho_A c_A^2} + \mathcal{O}\left([P]^2\right), \tag{2}$$

respectively, where $\rho = 1/v$ is the density, s the specific entropy, T the temperature and $M = \|\mathbf{u}\|/c$, in which $\mathbf{u}$ is the velocity and $c = \sqrt{(\partial P/\partial\rho)_s}$ the speed of sound. The thermodynamic parameter Γ is defined as

$$\Gamma = 1 + \frac{\rho}{c}\left(\frac{\partial c}{\partial \rho}\right)_s \tag{3}$$

and is known as the fundamental derivative of gasdynamics for the special role it plays in many areas of compressible fluid dynamics [4]. If $\Gamma > 1$, which is true for example for ideal gases with constant specific heats ($\Gamma = (\gamma+1)/2$, where $\gamma > 1$ is the ratio of the specific heats), the speed of sound increases if the substance is compressed isentropically.

By substituting the definition of the speed of sound into the expression for Γ, it is easily seen that if $\Gamma > 0$, the isentropes are convex in the pressure–specific volume plane. For weak shocks ($[P]$ sufficiently small), Eq. (1) shows that, if $\Gamma > 0$, only compression shocks satisfy $s_B \geq s_A$, as required by the second law of thermodynamics. Conversely, if $\Gamma < 0$, expansion shocks are admissible rather than compression shocks. Expansion shocks are an example of *non-classical* shock waves; here the term non-classical indicates the reversed, unconventional character of the shock wave (more in general, the gasdynamics in the regime $\Gamma < 0$ is referred to as non-classical gasdynamics).

Eq. (2) shows that the Mach number does not necessarily decrease across the shock as in perfect gases. Note that the normal Mach number, u_n/c, formed using the velocity component perpendicular to the shock front, instead always decreases across admissible shocks (in accordance with speed ordering stability criterion, see [5]). If $\Gamma < 1$, the speed of sound can decrease across a compression shock and in a sufficient amount to compensate the decrease of the velocity magnitude, resulting in an overall increase of the Mach number. For a weak shock, $M_B > M_A$ is realized if the upstream state is such that $1 - \Gamma - 1/M^2$ is positive. Following the nomenclature introduced by Vimercati et al. [3], we refer to Mach number–increasing shocks as *non-ideal* oblique shocks.

In the present work, the conditions for the formation of non-ideal and non-classical shock waves are reviewed. Finite-amplitude shocks will be considered, i.e. the assumption of weak shocks, used in this section for introduction purposes and useful to delineate existence conditions, is dropped in the following. As a result, specific domains are reported in which the state upstream of the shock must be located in order that any of the aforementioned non-ideal phenomena can be observed. Moreover, selected mechanisms of non-classical shock interaction are discussed.

Thermodynamic states featuring $\Gamma < 1$ can be found in the vapour-liquid equilibrium region in the neighbourhood of the critical point [7] or in the single-phase vapour

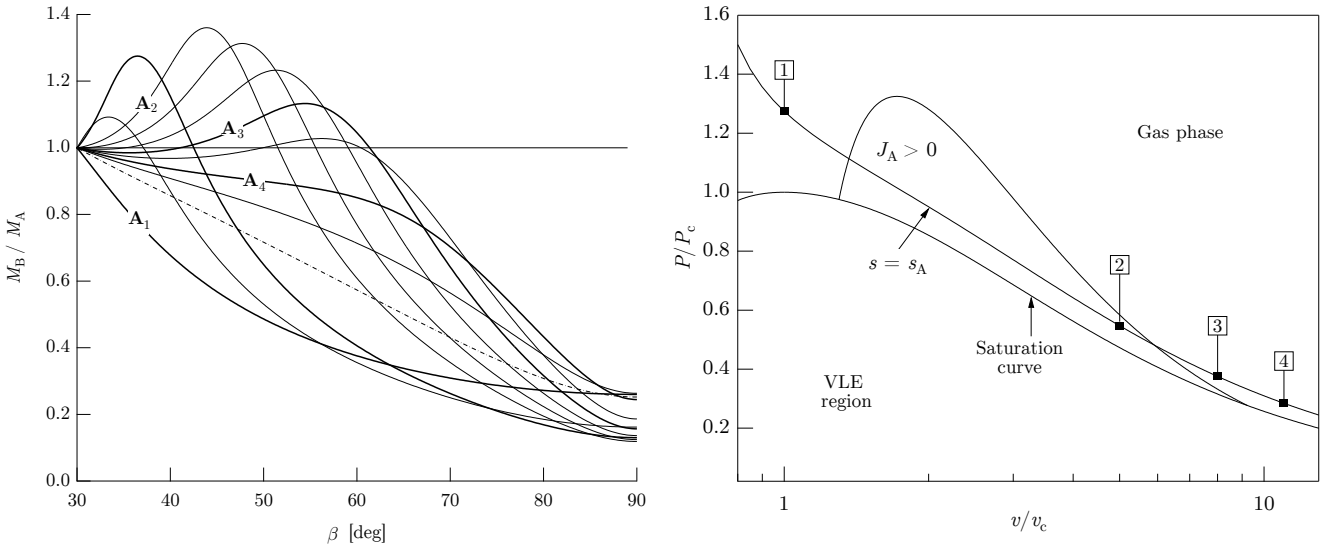

Figure 1: Shock curves for MDM in the post-shock Mach number–shock angle plane (thermodynamic properties from REFPROP [6]). The pre-shock Mach number is fixed to $M_A = 2$. The pre-shock thermodynamic states are selected along the same isentrope $s_A = s(1.2743P_c, v_c)$ crossing the region $J_A > 0$ (subscript c for critical-point quantities). Marked configurations: $v_1 = v_c$, $v_2 = 5v_c$, $v_3 = 8v_c$, $v_3 = 11v_c$. Also shown is the ideal gas limit (dash-dotted curve).

region of molecularly complex fluids, near to the saturation curve and critical point [8]. In this study, the focus is on the latter class of fluids; in particular, when discussing non-classical shock waves, so-called Bethe-Zel'dovich-Thompson fluids or briefly BZT fluids (from the names of the pioneers of this field) are considered.

The structure of this work is as follows. In §2, non-ideal oblique shocks featuring an increase of the Mach number are examined in the classical gasdynamic context. Section §3 presents the non-classical theory of oblique shock waves, within a generalised framework of oblique wave curves (shock polars in the classical context). Possible ways in which non-classical oblique shocks interact producing further non-classical waves are discussed in §4. Section 5 outlines the concluding remarks.

2 Non-ideal oblique shock waves

As the Mach number is a parameter of primary interest in many applications, the potential increase of the Mach number across oblique shock waves is among the most significant shock-related non-ideal effects. Analysis of the isentropic limit of weak compression shock waves (Eq. (2)) demonstrates that oblique shock waves in which the post-shock Mach number is larger than the pre-shock Mach number are indeed admissible if $\Gamma < 1$. In the following we show how non-ideal oblique shocks of finite amplitude arise. For simplicity, the analysis if restricted to fluids exhibiting $\Gamma > 0$ in the gaseous phase. To this end, selected shock parameters are varied, clarifying in particular the role of the pre-shock thermodynamic state at a given pre-shock Mach number. The fluid used in this section for illustrative purposes is MDM (ocatmethyltrisiloxane, $C_8H_{24}0_2Si_3$), modelled via the REFPROP library [6].

Figure (1) shows the variation of the post-shock Mach number with the shock angle β (i.e. the angle formed by the shock front and the pre-shock flow direction) for a fixed pre-shock Mach number $M_A = 2$ and different pre-shock thermodynamic states selected along the same isentrope s_A crossing the region $J_A > 0$, where $J = 1 - \Gamma - 1/M^2$ using the notation of Cramer & Best [9]. With the pre-shock Mach number fixed, the locus $J_A = 0$ shown in figure Figure (1) coincides with the isoline $\Gamma = 1 - 1/M_A^2$. Four pre-shock thermodynamic states are now considered, as representative of the possible qualitative evolution of the post-shock Mach number along the shock curve

State A_1 is located at higher densities than those characterising the region $J_A > 0$. In this case, the post-shock Mach number monotonically decreases with increasing shock angle. Exemplary non-monotonic Mach number distributions are those corresponding to pre-shock states A_2 and A_3 in Figure (1). State A_2 is taken as representative of the Mach number evolution for pre-shock states featuring $J_A > 0$. For increasing shock angles starting from $\beta = \sin^{-1}(1/M_A)$, the post-shock Mach number increases. As the magnitude of the tangential velocity decreases (i.e. with increasing shock angle), the post-shock Mach number reaches a local maximum and subsequently decreases towards the subsonic values characterizing strong oblique shocks.

If the pre-shock state exhibits $J_A < 0$, yet the thermodynamic state is selected in the close proximity of the region $J_A > 0$, such as case A_3 shows, the post-shock Mach number features a non-monotonic profile comprising two stationary points. The Mach number initially decreases as required by Eq. (2), but subsequently increases as the post-shock speed of sound decreases enough to compensate the change in the velocity magnitude.

By increasing the pre-shock specific volume along the reference isentrope, the two stationary points found in A_3-like configurations occur at $M_B < M_A$ and ultimately become coincident. Therefore, any further increase in v_A is such that the post-shock Mach number monotonically decreases with increasing shock angle (despite a somewhat anomalous, non-ideal curvature of the Mach number distribution can be observed close to the region $J_A > 0$).

If the flow conditions resulting in the non-ideal Mach number increase across oblique shocks are collectively

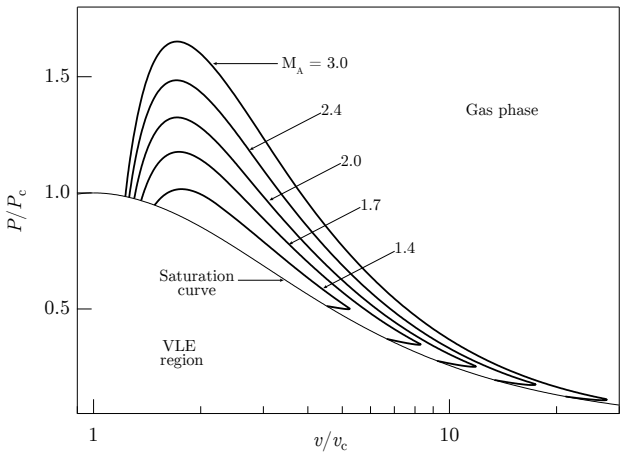

Figure 2: Existence domains of non-ideal oblique shocks in MDM (thermodynamic properties from REFPROP [6]). For a given pre-shock Mach number, the region enclosed between the corresponding locus in the gaseous phase and the saturation curve embeds all the pre-shock thermodynamic states from which non-ideal oblique shocks can occur.

considered, a domain of existence of non-ideal oblique shocks in the parameter space of pre-shock thermodynamic states and Mach number can be defined. If the pre-shock state lies in this domain, there exists at least one value of the shock angle leading to $M_B > M_A$. For a given pre-shock Mach number and for each value of the pre-shock entropy, the limit values of the pre-shock pressure or density, that bound the range where the shock curve possibly exhibits $M_B > M_A$ for some values of the shock angle, are computed. These limiting thermodynamic states define a locus embedding the region in which the pre-shock thermodynamic state must be selected (together with the given M_A) in order to observe a non-ideal oblique shock. As the pre-shock Mach number is varied, this procedure determines a one-parameter family of thermodynamic regions embedding all the pre-shock states from which non-ideal oblique shock can possibly occur [3].

Figure (2) reports the existence domain of non-ideal oblique shocks in the pressure–specific volume digram, for selected pre-shock Mach numbers. Each domain is represented by the region between the saturation curve and the limit curve corresponding to a given Mach number. For the most part, the domain associated with a given value of M_A coincides with the isoline $\Gamma = 1 - 1/M_A^2$ [3]. As a result, the domains are similar in shape to each other and their extension decreases as the pre-shock Mach number decreases. The existence domain of non-ideal oblique shocks shrinks as the pre-shock Mach number approaches the limit value $M_{A,min} = (1-\Gamma_{min})^{-1/2}$, where Γ_{min} denotes the minimum values of the fundamental derivative in the gaseous phase. For $M_A < M_{A,min}$, non-ideal oblique shocks are not possible.

3 Non-classical oblique shock waves

The most prominent example of non-classical oblique shock waves is undoubtedly the expansion oblique shock as predicted in the weak limit by Eq. (1) if $\Gamma_A < 0$. If finite-amplitude shocks are considered, the possibility that Γ changes sign has interesting consequences not only on expansion shocks, but also on compression shocks, due to the appearance of so-called sonic shocks, i.e. shocks having normal Mach number $M_n = u_n/c$ equal to 1 in either the pre-shock state (pre-sonic shock) or the post-shock state (post-sonic shock) or both states (double sonic shock) [10].

In contrast to the classical shock theory, in the non-classical context the presence of sonic shocks implies that the shock curves, i.e. the locus of post-shock state that can be connected to a given pre-shock state, may be discontinuous. It is instructive to examine this problem in the framework of the ramp/wedge problem, where a uniform supersonic stream with known properties is suddenly deflected by a ramp/wedge. The problem consists in finding the wave providing the turning of the uniform stream together with its downstream state, for a given ramp angle Θ. The solution set of the ramp problem is known as a wave curve, namely the locus of downstream states that can be connected to the given upstream state by means of wave originating in the corner of the ramp (scale invariance). In the classical gasdynamic context, the compression branch of the wave curve is the well-known shock polar [1]. If BZT fluids are considered, the structure of the wave curves becomes more complicated and exhibit a multitude of configurations.

Figure (3) illustrates the possible structure of non-classical wave curves in the downstream pressure–deflection diagram associated with a ramp/wedge, according to the classification of Vimercati et al. [11] The van der Waals gas model with $c_v/R = 57.69$, where c_v is the isochoric specific heat and R the gas constant, is used in this section. Non-classical shock waves can be found either in the compression or the expansion side of the wave curve. The wave-curve branches comprising non-classical shocks are described in the following.

Case $\mathcal{N}_1$ features classical oblique shocks for sufficiently small deflections (which implies $\Gamma_A > 0$). Increasing Θ causes the downstream normal Mach number to decrease until a post-sonic oblique shock is formed. To continue the compression, a post-sonic shock followed by an adjacent compression fan centred on the corner of the ramp/wedge is required. The fan is indeed the type of wave that makes the compression of a uniform sonic or supersonic stream possible in the $\Gamma < 0$ regime. As the ramp angle increases, the amplitude of the compression fan increases, until $\Gamma = 0$ at the end of the fan. Compression beyond this point requires the inclusion of another sonic shock, this time with pre-shock sonic state; the overall configuration is denoted as a shock-fan-shock compression wave. With increasing ramp angles, the compression fan becomes weaker and ultimately disappears, thereby recovering the configuration with a single non-sonic oblique shock. Type-$\mathcal{N}_2$ and type-$\mathcal{N}_3$ curves are generated if the upstream thermodynamic state is inside the negative-Γ region. As a result, for small deflection angles, an inverted behaviour is observed. For increasing downstream pressures, the compression is first realised by a centred fan, until $\Gamma = 0$ at the downstream state and a pre-sonic oblique shock must be inserted to continue the compression (fan-shock compression wave). The largest compressions are accomplished by conventional oblique shocks; the boundary between these two branches is a pre-sonic shock solution. Given that $\Gamma_A < 0$, non-classical oblique shocks are of course found also in the expansion branch. Here, expansion oblique shocks are observed for the entire range of deflection angles (case $\mathcal{N}_2$) or for a range of deflection angles only (case $\mathcal{N}_3$) until $M_n = 1$ on the post-shock state and

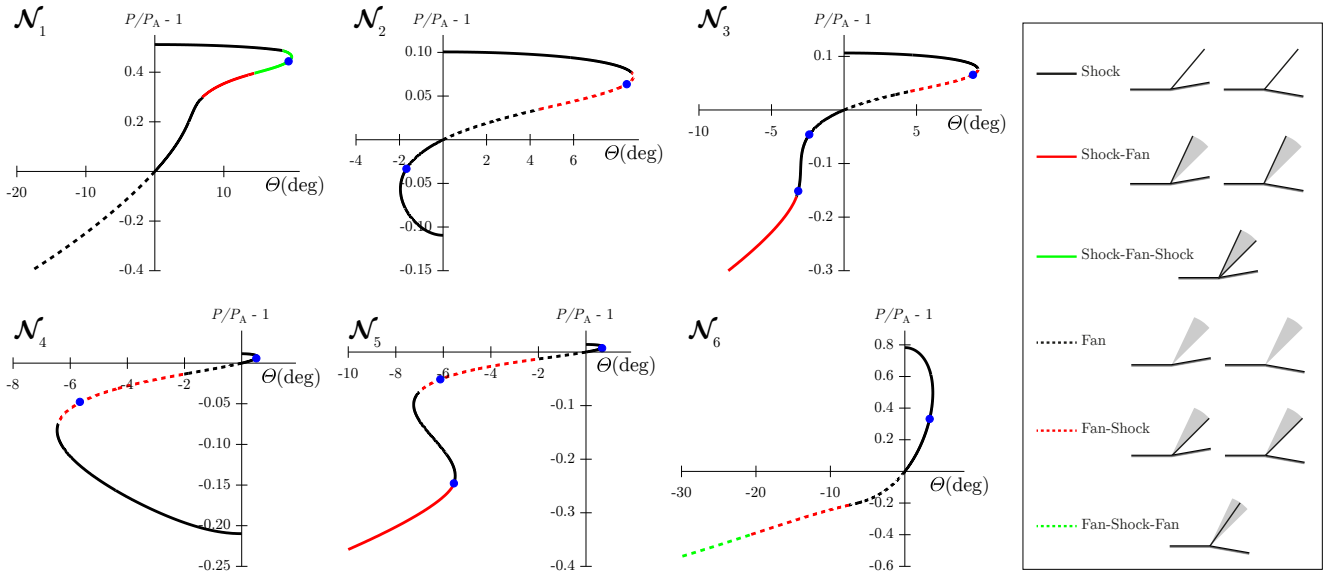

Figure 3: Pressure-deflection diagrams for centred oblique waves in the ramp problem for a van der Waals gas ($c_v/R = 57.69$). The upstream states are all selected along the same isentrope $s_A = s(0.74P_c, 2.5v_c)$; the upstream specific volume and Mach number are ($\mathcal{N}_1$) $v_A = 2.5v_c$, $M_A = 1.09$; ($\mathcal{N}_2$) $v_A = 1.3v_c$, $M_A = 1.08$; ($\mathcal{N}_3$) $v_A = 1.3v_c$, $M_A = 1.1$; ($\mathcal{N}_4$) $v_A = v_c$, $M_A = 1.08$; ($\mathcal{N}_5$) $v_A = v_c$, $M_A = 1.1$; ($\mathcal{N}_6$) $v_A = 0.7v_c$, $M_A = 1.6$. Symbol • for downstream sonic states.

a fan is required to continue the expansion (shock-fan expansion wave).

Curves $\mathcal{N}_4$ and $\mathcal{N}_5$, for which $\Gamma_A > 0$, include non-classical waves in the expansion branch only. Non-classical shocks are observed after the initial fan reaches the condition $\Gamma = 0$; the expansion is continued by inserting a pre-sonic oblique shock (fan-shock expansion wave). The fan becomes weaker with decreasing ramp angles until it disappears and a single expansion oblique shock provides the deflection. For type-$\mathcal{N}_5$ curves, the expansion shock ultimately features $M_n = 1$ in the post-shock state and an additional shock-fan expansion wave provides the strongest expansions. Finally, curves of type $\mathcal{N}_6$ ($\Gamma_A > 0$) are distinguished by the following sequence of oblique waves along the expansion branch, in the order of decreasing downstream pressure: fan, fan-shock, fan-shock-fan. Here the fan-shock-fan waves are characterised by the presence of a double-sonic shock between the two centred fans.

As the choice of the upstream states in Figure (3) demonstrates, for certain upstream thermodynamic states, two different types of wave curves are possible depending on the value of the upstream Mach number. Based instead on the upstream thermodynamic state only, the non-classical wave curves can be grouped as follows: $\mathcal{N}_1$, $\mathcal{N}_2/\mathcal{N}_3$, $\mathcal{N}_4/\mathcal{N}_5$, $\mathcal{N}_6$. A procedure for determining the transition between each of this groups is detailed by Vimercati et al [11]. It is based on detecting, for any given value of the upstream entropy, limiting values of the pressure or density (for example, the $\Gamma = 0$ locus for the group $\mathcal{N}_2/\mathcal{N}_3$ or the so-called double sonic locus [12] for the transition between the $\mathcal{N}_4/\mathcal{N}_5$ and the $\mathcal{N}_6$ groups). The result of the procedure is a map, shown in Figure (4) in the P–v plane, of upstream states associated with each type of wave curve. It is seen that the region of upstream thermodynamic states leading to non-classical wave curves is significantly larger than the $\Gamma < 0$ region and covers a wide range of states for which $s_{vle} < s_A < s_\tau$, where s_{vle} and s_τ denote the isentrope tangent to the saturation curve and $\Gamma = 0$ locus, respectively. Outside the non-classical region, only type-$\mathcal{C}$ curves (i.e. the classical wave curves composed of oblique shocks/centred fans in the compression/expansion branch) are generated. For the regions of upstream thermodynamic states where two different configurations are possible, the following holds: type-$\mathcal{C}$, $\mathcal{N}_2$ and $\mathcal{N}_4$ curves occur if $M_A < M_A^{tr}$; $\mathcal{N}_1$, $\mathcal{N}_3$ and $\mathcal{N}_5$ curves are observed if $M_A > M_A^{tr}$, where M_A^{tr} is the transitional Mach number which depends on the upstream thermodynamic state.

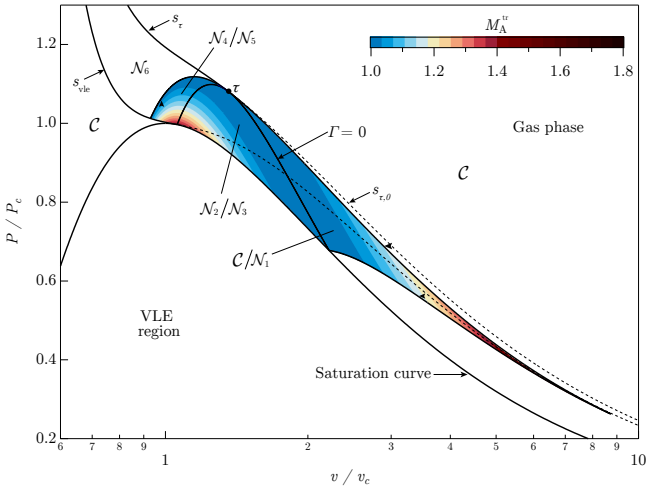

Figure 4: Upstream-state map of the wave curves in the P–v for a van der Waals gas with $c_v/R = 57.69$. Superposed is the value of transitional upstream Mach number for the regions where two different configurations are possible.

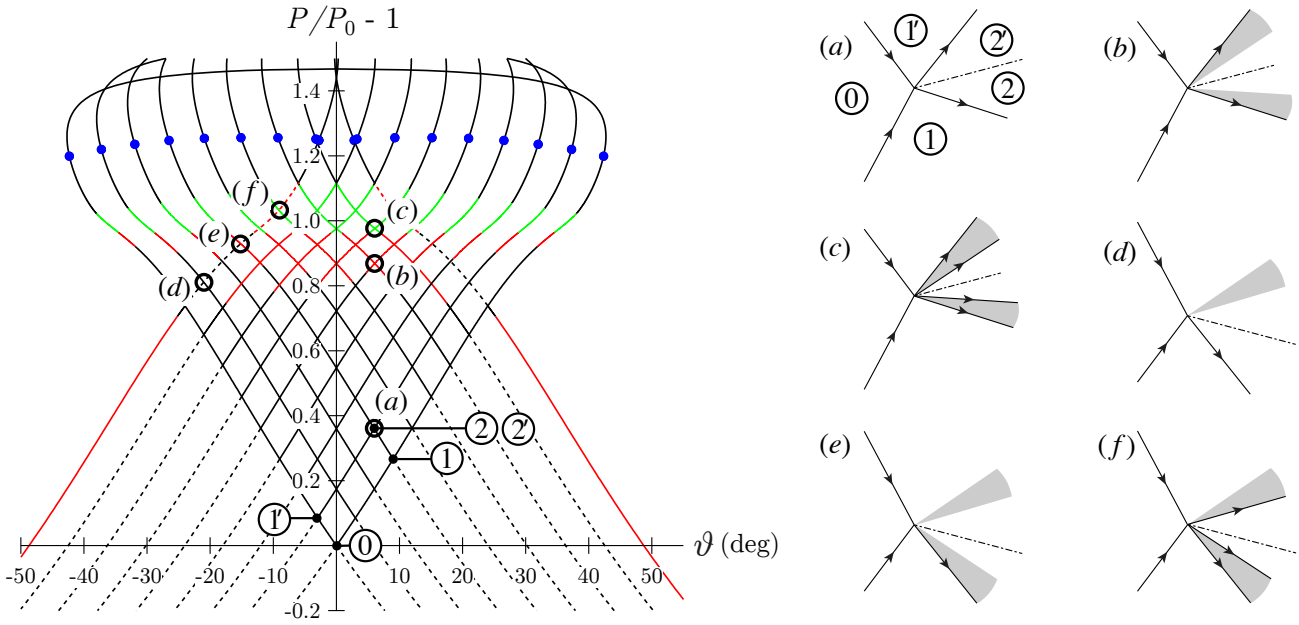

Figure 5: Pressure–deflection diagram for the crossing of compression shocks in a polytropic van der Waals gas ($c_v/R = 57.69$) and schematic illustrations of the cross-node patterns (upstream flow from left to right). Only oblique compression waves are generated in this type of interaction. Upstream state: $P_0 = 0.527P_c$, $v_0 = 4v_c$, $M_0 = 1.5$. Same conventions for the wave curves as in Figure (3).

4 Non-classical interactions of oblique shock waves

The existence of non-classical waves for supersonic flow over a ramp/wedge implies that non-classical waves can also be generated by the crossing, overtaking and splitting of compression and expansion oblique shocks. Restricting the analysis to node patterns, i.e. to the immediate neighbourhood of the interaction point in a scale-invariant flow, makes it possible to directly use the wave curves computed for the ramp/wedge problem to predict the outgoing waves of the interaction, for a given couple of incoming shock waves. This is the classical method of the wave curves [13], which we apply here to non-classical flow solutions. A detailed analysis of shock interactions in BZT fluids can be found in [14]; in this section some of the most relevant configurations are discussed.

Figure (5) shows a pressure–deflection diagram for a cross-node (two shocks travelling in opposite directions collide) in the same van der Waals gas used in the previous section. Two incident wave curves (one for each propagation direction of the incoming shocks) and a number of reflected wave curves (i.e. computed from the state immediately downstream of an incident wave) are reported. As an example, two shocks travelling in a uniform supersonic stream (state 0) result in state 1 and 1' of the flow. In order to turn the flow to a final common direction, two additional shocks are generated, which cause a further jump to states 2 and 2' separated by a contact discontinuity. The outgoing wave are determined by the intersection of the reflected wave curves, as the pressure and flow direction must match across the contact discontinuity emanating from the node.

In Figure (5), both incident shocks are compression shocks; as the graphical analysis shows, only compression waves can be generated in this type of interaction. Case *a* depicts the typical configuration of a cross node in classical gasdynamics. Two incident compression shocks produce two outgoing shocks with a slip line in between.

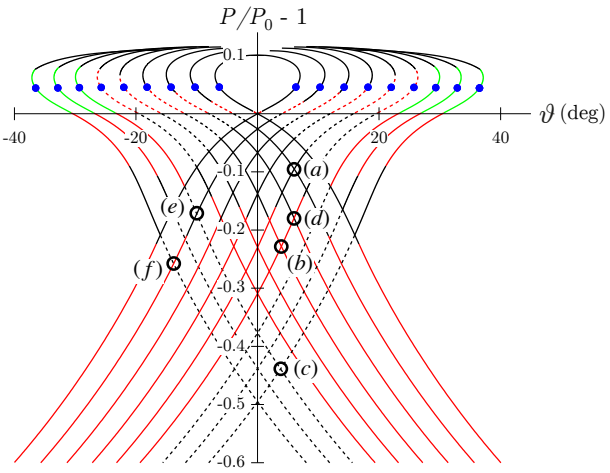

Figure 6: Pressure–deflection diagram for the crossing of expansion shocks in a polytropic van der Waals gas ($c_v/R = 57.69$) and schematic illustrations of the cross-node patterns (upstream flow from left to right). Only oblique expansion waves are generated in this type of interaction. Upstream state: $P_0 = 1.032P_c$, $v_0 = 1.1v_c$, $M_0 = 1.5$. Same conventions for the wave curves as in Figure (3).

By increasing the strength of the incident shocks, the intersection of the reflected wave curves occurs along the non-classical branches, implying that non-classical outgoing waves can be observed. Cases b and c are two such examples, which involve outgoing shock-fan and shock-fan-shock waves, respectively. Qualitative changes in the wave-structure across the incoming shocks are also possible, see cases d-f, further confirming that a wide variety of interaction patterns is to be expected in BZT fluid flows.

The crossing of expansion shocks is illustrated in Figure (6). Here, only expansion waves can be generated at the node. For relatively small pressure jumps across the incident shocks, it is seen that the interaction produces outgoing expansion shocks (case a). However, for larger pressure jumps more complicated configurations are necessary, such as a couple of expansion shock-fan waves (b) or pure fans (c). As for the case of compression shocks, transitions in the wave-curve structure play an important role and allow for the combination of expansion shock and shock-fan wave (d), shock and pure fan (e), fan and shock-fan wave (f) to be generated at the cross-node.

It should also be noticed that for a perfectly symmetric incident shock configuration, the outgoing wave pattern is also symmetric and the velocity and entropy jumps across the slip line vanish. Therefore, the flow configuration in each of the half planes about the symmetry axis is identical to that of a regular reflection.

5 Conclusions

Oblique shocks in the regime $\Gamma < 1$ may exhibit significant differences compared to oblique shocks in the ideal-gas regime, due to the peculiar variation of the speed of sound along the shock adiabat. Two classes of oblique shocks in single-phase gases were reviewed in this work.

Firstly, non-ideal oblique shocks, for which the Mach number increases from the pre-shock to the post-shock state, were investigated for thermodynamic states in the range $0 < \Gamma < 1$. In order to observe non-ideal oblique shocks, it is necessary that $1 - \Gamma - 1/M^2 > 0$ either in the pre-shock state or along the shock curve.

Next, non-classical oblique shock occurring the mixed regime where Γ can be either positive or negative were studied. The prototypical problem of a supersonic flow over a ramp/wedge served as a framework for the generalisation of the classical theory of the wave curves to the non-classical context. Non-classical oblique shocks, which include expansion shocks and sonic shocks (these can be both compression and expansion shocks), characterise the branches of the wave curves crossing the $\Gamma < 0$ region. Non-classical wave curves can be classified into six configurations and are expected to occur for a wide range of state located along isentropes crossing the negative-Γ region.

Finally, on the basis of the wave-curve analysis, interactions of oblique shocks in the cross-node configuration were analysed. It was shown that the collision of oblique compression shocks travelling in the opposite directions can easily generate non-classical sonic shocks and that the collision of oblique expansion shocks in most situations produces other expansion shocks.

Acknowledgment

This research is supported by ERC Consolidator Grant N. 617603, Project NSHOCK, funded under the FP7-IDEAS-ERC scheme.

References

[1] P. A. Thompson, *Compressilbe Fluid Dynamics*. McGraw-Hill, 1988.

[2] H. A. Bethe, "The theory of shock waves for an arbitrary equation of state," Technical paper 545, Office Sci. Res. & Dev., 1942.

[3] D. Vimercati, G. Gori, and A. Guardone, "Non-ideal oblique shock waves," *J. Fluid Mech.*, vol. 847, pp. 266–285, 2018.

[4] P. A. Thompson, "A fundamental derivative in gasdynamics," *Phys. Fluids*, vol. 14, no. 9, pp. 1843–1849, 1971.

[5] P. D. Lax, "Hyperbolic systems of conservation laws II," *Commun. Pur. Appl. Math.*, vol. 10, no. 4, pp. 537–566, 1957.

[6] E. W. Lemmon, M. L. Huber, and M. O. McLinden, "NIST reference database 23: reference fluid thermodynamic and transport properties–REFPROP, version 9.1," *Standard Reference Data Program*, 2013.

[7] N. R. Nannan, C. Sirianni, T. Mathijssen, A. Guardone, and P. Colonna, "The admissibility domain of rarefaction shock waves in the near-critical vapour-liquid equilibrium region of pure typical fluids," *J. Fluid Mech.*, vol. 795, pp. 241–261, 5 2016.

[8] P. Colonna and A. Guardone, "Molecular interpretation of nonclassical gasdynamics of dense vapors under the van der Waals model," *Phys. Fluids*, vol. 18, no. 5, pp. 056101–1–14, 2006.

[9] M. S. Cramer and L. M. Best, "Steady, isentropic flows of dense gases," *Phys. Fluids A*, vol. 3, no. 4, pp. 219–226, 1991.

[10] A. Kluwick, "Rarefaction shocks," in *Handbook of Shock Waves* (G. Ben-Dor, O. Igra, and T. Elperin, eds.), pp. 339–411, Academic Press, 2001.

[11] D. Vimercati, A. Kluwick, and A. Guardone, "Oblique waves in steady supersonic flows of Bethe-Zeldovich-Thompson fluids," *J. Fluid Mech.*, vol. 855, pp. 445–468, 2018.

[12] C. Zamfirescu, A. Guardone, and P. Colonna, "Admissibility region for rarefaction shock waves in dense gases," *J. Fluid Mech.*, vol. 599, pp. 363–381, March 2008.

[13] J. Glimm, C. Klingenberg, O. McBryan, B. Plohr, D. Sharp, and S. Yaniv, "Front tracking and two-dimensional Riemann problems," *Advances in Applied Mathematics*, vol. 6, no. 3, pp. 259–290, 1985.

[14] D. Vimercati, A. Kluwick, and A. Guardone, "Shock interactions in two-dimensional steady flows of Bethe-Zeldovich-Thompson fluids," *J. Fluid Mech.*, vol. 887, 2020.